Bioorganic Chemistry 36 (2008) 169–177

Contents lists available at ScienceDirect

Bioorganic Chemistry

journal homepage: www.elsevier.com/locate/bioorg

Stereospecificity, substrate, and inhibitory properties of nucleoside diphosphate analogs for creatine and pyruvate kinases

Charlotta K. Wennefors, Mikhail I. Dobrikov, Zhihong Xu, Ping Li [1], Barbara Ramsay Shaw *

Department of Chemistry, French Family Science Center, Duke University, 124 Science Drive, Durham, NC 27708-0354, USA

ARTICLE INFO

Article history:
Received 25 January 2008
Available online 22 April 2008

Keywords:
Creatine kinase
Pyruvate kinase
α-*P*-borano phosphate
Phosphonate
Negative cooperativity
TSAC
Kinetics

ABSTRACT

Antiviral α-*P*-borano substituted NTPs are promising chain terminators targeting HIV reverse transcriptase (RT). Activation of antiviral nucleoside diphosphates (NDPs) to NTPs may be carried out by pyruvate kinase (PK) and creatine kinase (CK). Herein, are presented the effects of nucleobase, ribose, and α-phosphate substitutions on substrate specificities of CK and PK. Both enzymes showed two binding modes and negative cooperativity with respect to substrate binding. The stereospecificity and inhibition of ADP phosphorylation by α-*P*-borano substituted NDP (NDPαB) stereoisomers were also investigated. The *Sp*-ADPαB isomer was a 70-fold better substrate for CK than the *Rp* isomer, whereas PK preferred the *Rp* isomer of NDPαBs. For CK, the *Sp*-ADPαB isomer was a competitive inhibitor; for PK, the *Rp*-ADPαB isomer was a poor competitive inhibitor and the *Sp*-ADPαB isomer was a poor non-competitive inhibitor. Taken together, these data suggest that, although the *Rp*-NDPαB isomer would be minimally phosphorylated by CK or PK, it should not inhibit either enzyme.

1. Introduction

Nucleoside analogs targeting retroviral reverse transcriptases (RTs) are an important class of antiviral agents [1–4]. The need for these analogs to undergo metabolic conversion to be biologically active [1,4,5] has lead to problems such as poor phosphorylation by intracellular kinases [3,5,6] and undesired metabolic effects [7,8]. Another disadvantage of existing nucleoside analogs is the eventual emergence of drug resistance [4,9–12]. It has been demonstrated that α-*P*-borano modifications in clinically relevant dideoxy NTPs (ddNTPs) such as AZT, d4T [2], ddA [4,10], and acycloT [13] improve their incorporation into viral DNA by wildtype HIV-1 RT [2], and even more so by mutant drug resistant HIV-1 RTs [4,10] and MMLV RT [13,14]. Furthermore, after incorporation into viral DNA, the *Rp* isomers of α-*P*-borano substituted AZT-TP and d4T-TP have demonstrated increased stability toward the ATP-dependent repair mechanism that contributes to drug resistance [2,4,10]. Thus α-*P*-borano nucleotide analogs are promising antiviral candidates for selectively targeting mutant RTs.

In boranophosphates analogs, one of the non-bridging oxygens on the α-phosphate of nucleoside mono- (NMP), di- (NDP), or triphosphates (NTPs) is replaced by a borane $-BH_3^-$ group (Fig. 1) [15–26].

The borane group is isoelectronic with oxygen in normal phosphate, isolobal with sulfur in phosphorothioates, and isosteric with the methyl group in methylphosphonates [15–24]. Whereas the boranophosphates share the same net charge and geometry about the phosphorus as unmodified phosphates, the boranophosphates have a longer P–B bond than the P–O bond in normal phosphate (1.91 versus 1.51 Å), a reduced tendency to coordinate metal ions or form H bonds, and an altered polarity [27]. The lower electronegativity of boron (2.04) than the oxygen (3.44) in a phosphodiester bond [27,28] gives reason to the observation that α-*P*-borano phosphate groups accelerate the incorporation of chain terminators into viral DNA [2,4,10,14,26,29], resulting in the increased potency of these drugs. Ultimately, however, the potency of these nucleotide analogs as antiviral drugs is highly dependent on their phosphorylation by host cellular kinases. To circumvent one or two steps involved in the activation of ddNTPαBs, prodrugs of ddNMPαB and ddNDPαB were recently developed [13,30,31]. Despite these efforts, the last step in the phosphorylation of

Abbreviations: CK, creatine kinase; PCr, creatine phosphate; PK, pyruvate kinase; PeP, phosphoenolpyruvate; NDPK, nucleoside diphosphate kinase; TSAC, transition state analog complex; TS, transition state; N, nucleoside; NDP, nucleoside diphosphate; NTP, nucleoside triphosphate; dNTP, deoxynucleoside triphosphate; ddNTP, 2′,3′-dideoxynucleoside triphosphate; ddNTPαB, α-*P*-borano substituted 2′,3′-dideoxynucleoside triphosphate; ATPαB, α-*P*-borano substituted ATP; ATPαS, α-*P*-thio substituted ATP; AZT, 3′-deoxy-3′-azidothymidine; d4T, 2′,3′-dideoxythymidine; ddA, 2′,3′-dideoxyadenosine, acycloT, 1-(2-hydroxyethoxymethyl)-thymine; HIV, human immunodeficiency virus; NRTI, nucleoside reverse transcriptase inhibitor; HPLC, high performance liquid chromatography.

* Corresponding author. Fax: +1 919 660 1605.
E-mail address: barbara.r.shaw@duke.edu (B.R. Shaw).
[1] Present address: Department of Chemistry, Massachusetts Institute of Technology, 77 Massachusetts Avenue, Cambridge, MA 02139, USA.

0045-2068/$ - see front matter © 2008 Elsevier Inc. All rights reserved.
doi:10.1016/j.bioorg.2008.03.001

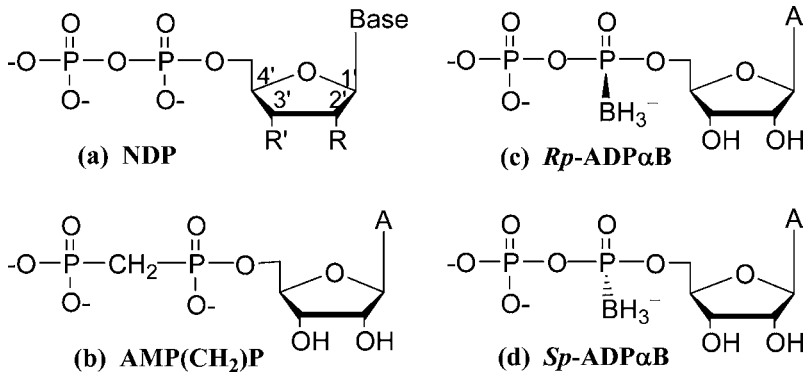

Fig. 1. Nucleoside diphosphate (NDP) ribose and α-*P* modifications. NDP: R = OH, R′ = OH; 2′-dNDP: R = H, R′ = OH; 3′-dNDP: R = OH, R′ = H; 2′,3′-ddNDP: R = H, R′ = H. α-*P* modifications: α,β-AMP(CH_2)P (bottom left). The *Rp*-ADPαB isomer (top right), and the *Sp*-ADPαB isomer (bottom right).

nucleoside analog diphosphates to their respective triphosphates remains largely unexplored [5].

Previous studies revealed that nucleoside diphosphate kinase (NDPK), a major enzyme for NDP phosphorylation in cells, phosphorylates AZT-DP, d4T-DP, and ddC-DP poorly [1,3,5,32]. Krishnan and co-workers evaluated the roles of creatine kinase (CK), 3-phosphoglycerate kinase (PGK), and pyruvate kinase (PK) in NDP analog phosphorylation and proposed that the specificity of the kinases toward the antiviral ddNDPs is dependent on both the configuration of the analog (L or D) and the presence of a 3′-hydroxyl group in the sugar moiety [5]. Furthermore, the researchers suggest that CK and PK may be responsible for the last phosphorylation step of 2′,3′-dideoxy- and acyclo-nucleoside diphosphates *in vivo* [5].

Previous studies by Meyer and co-workers indicated that α-*P*-borano substitutions on AZT-DP and d4T-DP enhance efficiency of phosphorylation by NDPK by 10-fold [2]. Although the catalytic efficiency was enhanced by the borano, it was still 1000-fold less than for the parent NDPs [2], suggesting that other kinases, perhaps CK or PK, might be more efficient enzymes for the phosphorylation of ddNDP to ddNTP. CK and PK have opposite stereospecificity for binding and phosphorylation of the *Rp* and *Sp* isomers of α-*P*-thio substituted NDPs [33]. It is therefore likely that the *Rp*- and *Sp*-stereoisomers of α-*P*-borano substituted NDPs will be recognized distinctly by these enzymes. Thus, it is of interest to study the effects of the NDPαB stereoisomers on phosphorylation and substrate specificity of CK and PK.

CK is endogenous to muscle tissues that require large energy fluxes [34,35] as well as to non-muscle cells [36]. The dimeric enzyme catalyzes the reversible reaction between ADP and phosphocreatine or ATP and creatine. PK is a tetrameric enzyme involved in the glycolytic pathway by catalyzing the transfer of a phosphate group from phosphoenolpyruvate to ADP, to yield pyruvate and ATP. The kinetic schemes for both CK and PK are initiated by direct binding of ADP and creatine phosphate (for CK) or phosphoenolpyruvate (for PK) to the enzyme, subsequent formation of the transition state involving a conformational change of the enzyme, followed by a rate limiting phosphate transfer reaction, and finally product release (Scheme 1).

In the present study, the binding affinities of the substrate analogs used in this study were determined by a fluorescence quenching assay using equilibrium titration. A transition state analog complex (TSAC) was evaluated to determine the affinity of the NDP substrate for the transition state (Fig. 2). For both CK and PK, the TSAC is formed when a nitrate ion, NO_3^- occupies the position of the transferable phosphate during the transition state of the enzyme catalyzed reaction as demonstrated previously for ADP [37–42].

Herein, we report the specificity of CK and PK toward nine different nucleobase, ribose, and α-phosphate substituted NDPs and the effect of the α-*P*-borano modification on the phosphorylation of NDPs (refer to Fig. 1). Substrate properties, inhibitory properties, and stereochemical effects of α-*P*-borano nucleoside diphosphates for CK and PK are also presented.

2. Materials and methods

2.1. Materials

Creatine, $NaNO_3$, Hepes, Bicine, KCl, sodium oxalate, glycerol, tryptophan methyl ester hydrochloride, creatine phosphate and nucleoside diphosphates (including AMP(CH_2)P) and triphosphates were obtained from Sigma–Aldrich. KOH was obtained from Fisher. $MgCl_2$ was obtained from Ambion. Rabbit muscle creatine kinase and rabbit muscle pyruvate kinase were purchased as desiccated powders from Roche. ADPαB and GDPαB were synthesized, purified, and the isomers were separated by HPLC as published previously [43].

2.2. Stock solutions

Concentrations of NDPs in 70 mM Hepes (pH 7) were determined by Cary UV–vis spectrophotometer and the purity was determined by Varian HPLC. For CK studies the direct binding (DB) buffer [38] was adjusted to pH 8.3 and contained 50 mM Bicine, 50 mM KCl, and 5 mM $MgCl_2$; the transition state analog complex (TSAC) binding buffer [38] was adjusted to pH 8.3 and contained 50 mM Bicine, 5 mM $MgCl_2$, 50 mM $NaNO_3$, and 20 mM creatine. For PK studies the direct binding buffer was adjusted to pH 7.5 and contained 50 mM Hepes, 5% glycerol, 5 mM $MgCl_2$, 2 mM sodium oxalate, and 100 mM KCl. The TSAC binding buffer was adjusted to pH 7.5 and contained 50 mM Hepes, 5% glycerol, 5 mM $MgCl_2$, 2 mM sodium oxalate, 50 mM KCl, and

$$\mathrm{E{:}PX + ADP} \overset{K_d^{ADP}}{\rightleftharpoons} \mathrm{E{:}PX{:}ADP} \overset{K'^{ADP}_d}{\rightleftharpoons} \left[\mathrm{E{:}PX{:}ADP}\right]^{\ddagger} \overset{k_p}{\rightleftharpoons} \mathrm{E{:}X{:}ATP} \overset{K_d^{ATP}}{\rightleftharpoons} \mathrm{E + X + ATP}$$

Scheme 1. CK and PK kinetic scheme. ADP and phosphate donor binds to the enzyme. A conformational change of the enzyme forming the transition state is followed by the rate limiting phosphate transfer, followed by product release. E = CK or PK, PX = creatine phosphate (for CK) or phosphoenolpyruvate (for PK), X = creatine (for CK) or pyruvate (for PK), ADP = adenosine diphosphate, and ATP = adenosine triphosphate.

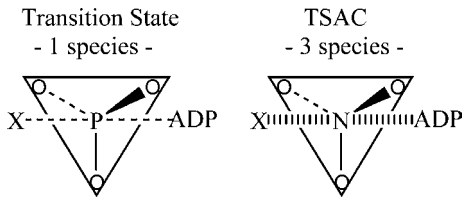

Fig. 2. The nitrate transition state analog complex (TSAC) is formed when NO_3^- occupies the position of the transferable phosphate, during the transition state of the enzyme catalyzed reaction. Three species; X (creatine or pyruvate), nitrate (right), and ADP are interacting through hydrogen bonding, mimicking the phosphoryl transition state (one complex) (left).

50 mM KNO_3. Fresh CK and PK stock solutions were prepared immediately prior to each kinetic experiment and kept on ice throughout the experiment. The enzyme concentrations were determined using the absorbance at 280 nm with extinction coefficients of 0.88 for 1 mg/mL CK (M_W = 81,000 g/mol) [44], and 0.54 for 1 mg/mL PK (M_W = 237,000 g/mol) [45]. The active enzyme concentration was determined using the specific activity of 200 μmol of ATP converted to ADP per min per mg of CK (forward reaction) at pH 9.0 and 30 °C [37,44], and 260 μmol pyruvate per min per mg of PK at pH 7.0 and 25 °C [46,47].

2.3. Affinity study

The affinities of the substrate analogs for direct and TSAC binding were determined with a fluorescence quenching assay using equilibrium titration. The solution of 1 μM CK, or 0.2 μM PK (for guanosine derivatives) or 0.7 μM PK (for adenosine derivatives) in "direct binding buffer" or "TSAC binding buffer" was titrated with NDP as in [38]. After each subsequent aliquot (0.25–10 μL) of stock NDP (or NTP) was added to the 1-mL buffer solution, the solution was allowed to equilibrate for approximately 1 min before fluorescence was measured in triplicate. All fluorescence measurements were made at 25 ± 1 °C. Excitation of tryptophan residues in CK or PK was carried out at 295 ± 2 nm and emission was measured at 340 ± 3 nm. A 4 μM solution of tryptophan methyl ester hydrochloride in deionized water was titrated with NDP for correction of collisional quenching and dilution.

The accumulated fluorescence values were converted to % quenching according to $Q = 100(F_0 - F/F_0)$, where F_0 is the initial fluorescence measured, and F is the fluorescence measured at a specific point. The readings were corrected (Q') for inner filter effects and Q'_{max} was determined by fitting the highest concentration data to the following Lineweaver–Burk equation,

$$1/Q' = (K_d/Q'_{max})(1/[S]) + 1/Q'_{max} \quad (1)$$

where Q' is the % quenching (corrected for inner filter effects), Q'_{max} is the maximum quenching, [S] is the substrate concentration, and K_d is the equilibrium dissociation constant for the substrate.

Each set of data for the fluorescence quenching experiment was then analyzed using the following Hill equation,

$$\log[Q'/(Q'_{max} - Q')] = n \log[S]_{free} - \log K_d \quad (2)$$

where Q' is the % quenching (corrected for inner filter effects) at a specific point, Q'_{max} is the maximum quenching, $[S]_{free}$ is the free substrate concentration ($[S]_{free} = [S]_{total} - [CK]_{total} * Q'/Q'_{max}$), n is the Hill coefficient, and K_d is the equilibrium dissociation constant for the substrate. By fitting the data to Eq. (2), the equilibrium dissociation constants, K_{d1} and K_{d2}, and the Hill coefficients, n_1 and n_2, were determined.

The difference in the binding free energy change ($\Delta\Delta G_b$) between the different nucleoside diphosphate analogs was calculated using the following equation,

$$\Delta\Delta G_b = -RT \ln(K_{d1\,ADP}/K_{d1\,NDP}) \quad (3)$$

where R is 8.314 J/mol K, T is 298 K, and $K_{d1\,ADP}$ and $K_{d1\,NDP}$ are the dissociation constants associated with the first binding mode of ADP and the corresponding NDP analog, respectively.

2.4. Steady-state kinetics

Initial NDP phosphorylation reactions were performed to determine enzyme concentrations and reaction times to be used in the steady-state kinetic experiments. Enzyme concentrations and reaction times were varied while keeping all other components constant. Substrate concentrations were kept at 200 μM in a reaction mixture containing 20 mM creatine phosphate, 50 mM Bicine, 5 mM $MgCl_2$, and 50 mM KCl, buffered to pH 8.3. The concentration of enzyme was varied from 0 to 200 nM. The enzyme was added to the reaction mixture to start the reaction. The reaction was quenched in a 100 °C water bath with subsequent filtering of the reaction mixture using Microcon centrifugal filter devices (NMWL: 30,000). The amount of conversion of NDP to NTP was determined using HPLC. Complete separation of NDPs and NTPs was observed on a C18 column using a 3–15% methanol gradient in 50 mM TEAA (triethyl ammonium acetate buffer, buffered to pH 6.8). Next, the mixture was allowed to react for different time points while keeping [enzyme] and [NDP] constant. The [enzyme] and reaction time was chosen (below 20% substrate conversion) where the product formation was linearly dependent so the product amount directly correlates with the steady-state rate of product formation.

For kinetic analysis the substrate concentration was then varied between 0 and 3 mM while keeping [CK] and reaction time constant. The steady-state kinetic data were fit to the Lineweaver–Burk equation (Eq. (4)), using SIGMAPLOT 9.0, to determine values for k_{cat} and K_m which then were used to determine the efficiency of phosphorylation for each of the substrates,

$$1/k_{cat\,(app)} = (K_m/k_{cat})(1/[S]) + 1/k_{cat} \quad (4)$$

where k_{cat} is the rate constant for the phosphorylation, [S] is the substrate concentration, and K_m is the Michaelis–Menten dissociation constant. Control experiments were performed to ensure NDPαB stability throughout enzyme quenching.

2.5. Inhibition study

For CK, 0–600 μM of *Rp*- or *Sp*-ADPαB isomer were added to the reaction mixture used for ADP (0–2 mM) phosphorylation (50 mM Bicine, 5 mM $MgCl_2$, 50 mM KCl, and 20 mM creatine phosphate, at pH 8.3). The reactions were quenched after 2 min in a 100 °C water bath and the reaction mixture was subsequently filtered using Microcon centrifugal filter devices (NMWL: 30,000). The product formation was determined with HPLC as described above.

For PK, 0–2 mM of the *Rp*- or *Sp*-ADPαB isomers were added to the reaction mixture used for ADP (0–3 mM) phosphorylation (100 mM Hepes, 125 mM KCl, 3 mM $MnCl_2$, 3% glycerol, and 2.5 mM phosphoenolpyruvate at pH 7.5). Here, PK was added at room temperature to initiate the reaction and quenched after 30 s by adding 10 μL of 10 mM 2′,4′-dinitrophenylhydrazine (DNPH) in 3 M HCl. After incubating for 10 min at 37 °C, 40 μL of 0.1 M EDTA in 3 M KOH was added. The UV–vis absorbance at 520 nm was determined after 10 min incubation at room temperature.

The data was analyzed on double reciprocal plots using SIGMAPLOT 9.0. The inhibitory constant, K_i, was calculated using the Lineweaver–Burk equation for competitive inhibition

$$1/k_{cat} = K_m/k_{cat}[(1 + [I]/K_i)(1/[S])] + 1/k_{cat} \quad (5)$$

and non-competitive inhibition,

$$1/k_{cat} = K_m/k_{cat}[(1 + [I]/K_i)(1/[S])] + [(1 + [I]/K_i)(1/k_{cat})] \quad (6)$$

where k_{cat} is the rate constant for the phosphorylation, [S] is the substrate (ADP) concentration, [I] is the inhibitor concentration (*Rp*-ADPαB or *Sp*-ADPαB), K_m is the Michaelis–Menten dissociation constant, and K_i is the inhibitory constant.

3. Results

3.1. Affinity of NDPs and NTPs for CK and PK

Equilibrium dissociation constants of direct binding and TSAC binding were determined for a wide range of substrates by monitoring the fluorescence quenching of the tryptophan residue near the active site (Trp227 for CK, Trp157 for PK) upon substrate binding. The Hill plots show that at very low and very high substrate concentrations the slopes (n_1, n_2) approach 1.0. Furthermore, all NDP and NTP substrates for both CK and PK (including PK-NTP binding results published previously [48]) have a slope corresponding to the Hill coefficient, n_H, of <1.0 (0.5–0.8) between the points corresponding to $0.3Q'_{max}$ and $0.7Q'_{max}$. By fitting each linear part of the Hill plot to the Hill equation (2), values for Hill coefficients (n_1 and n_2) and dissociation constants (K_{d1} and K_{d2}) were calculated.

In the sample graph shown (Fig. 3A), K_{d1} and K_{d2} for the *Sp*-ADPαB isomer were calculated as 35 μM and 525 μM for direct binding, and 275 μM and 1380 μM for binding to the TSAC, where NO_3^- is replacing and mimicking the PO_3^- in the TS. A collection of the first binding modes for NDPs bound to CK in the TSAC are compiled in Fig. 3B and all NDP substrate analog binding constants in Table 1.

Similar binding behavior was observed with PK. PK is a tetrameric enzyme that potentially could have four binding modes. Here, we observed the two first binding modes (Fig. 4A). K_{d1} and K_{d2} for the *Rp*-GDPαB isomer (Fig 4A) were calculated as 135 μM and 660 μM for direct binding, and 107 μM and 380 μM for binding to the PK-TSAC. The NDP substrate analog first binding modes are compiled in Fig. 4B and all binding constants are summarized in Table 2.

All dissociation constants (K_{d1}, K_{d2}) and differences in free energy change values, $\Delta\Delta G_b$, can be found in Tables 1–3. Complete tables including maximum quenching values (Q'_{max}) and Hill coefficients (n_1, n_2) can be found in Supplementary data.

3.2. Steady-state kinetics of phosphorylation of ADP and ADPαB isomers by CK and PK

In an effort to better understand the mechanism of phosphorylation of ADP and the effect of stereoisomers of ADPαB, the phosphorylation of NDPs was studied using steady-state kinetics. From the Lineweaver–Burk plots of the phosphorylation data obtained for ADP and the stereoisomers of ADPαB (Fig. 5), values for k_{cat} and K_m, were obtained and then used to determine the efficiency of phosphorylation for each of the substrates (Table 4).

The *Sp*-ADPαB isomer has a lower K_m than ADP ($K_{mADP\alpha B}$ = 8 μM, $K_{m\,ADP}$ = 67 μM) and a lower rate of phosphorylation ($k_{cat\,Sp\text{-}ADP\alpha B}$ = 0.03 s^{-1}, $k_{cat\,ADP}$ = 370 s^{-1}) (Table 4). The *Rp*-ADPαB isomer has a larger K_m (1000 μM) and a lower k_{cat} (0.06 s^{-1}) than ADP. While a similar study was carried out using PK, no measurable phosphorylation was observed for either isomer of ADPαB using PK.

3.3. ADPαB inhibition of ADP phosphorylation by CK and PK

Since the initial experiments showed that the *Rp* and the *Sp* isomer of ADPαB are only minimally phosphorylated by CK or PK, an inhibition assay was performed to determine if either stereoisomer has an inhibitory effect on the phosphorylation of normal ADP (Fig. 6).

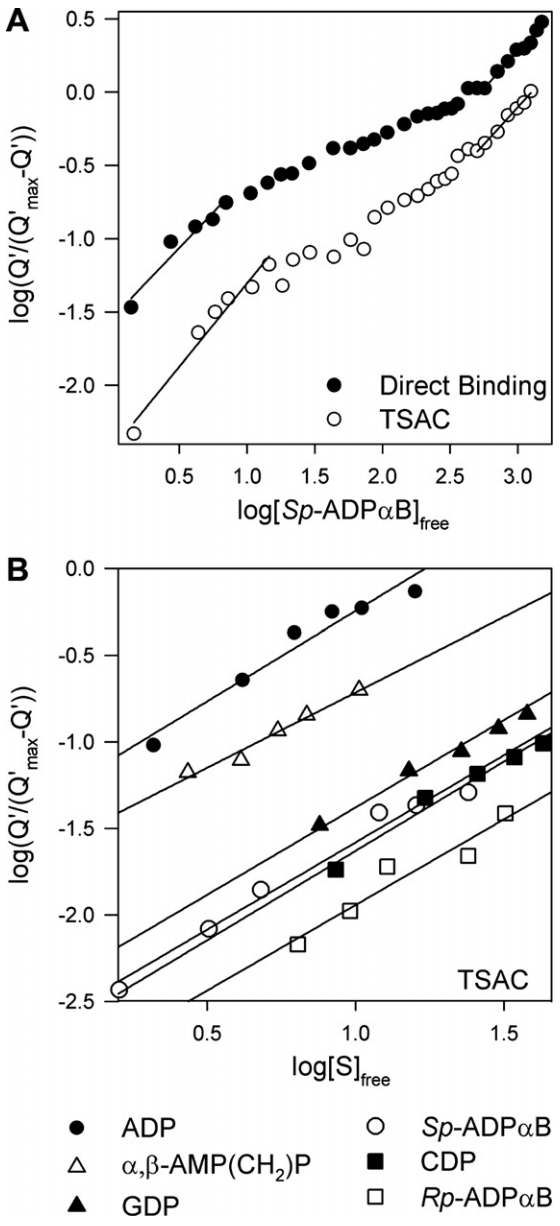

Fig. 3. (A) Hill plot of the *Sp*-ADPαB isomer for (•) direct binding and (○) TSAC binding with CK. (B) First binding mode of NDPs ((•) ADP, (Δ) α,β-AMP(CH_2)P, (▲) GDP, (○) *Sp*-ADPαB, (■) CDP, (□) *Rp*-ADPαB) bound to CK in TSAC. One micromolar CK in direct binding buffer (50 mM Bicine, 5 mM $MgCl_2$, and 50 mM KCl at pH 8.3) or TSAC binding buffer (50 mM Bicine, 5 mM $MgCl_2$, 50 mM $NaNO_3$, and 20 mM creatine at pH 8.3) was titrated with 0–2 mM NDP at 25 °C. Experiments were performed in triplicate.

For CK, the *Sp*-ADPαB isomer is a strong competitive inhibitor of the ADP reaction ($K_{m\,ADP}$ = 67 μM), as all extrapolations of these plots intersected on the *y*-axis with a K_i of 49 μM. However, for the *Rp*-ADPαB isomer, no CK inhibition is observed. In contrast, for PK, the *Rp*-ADPαB isomer is a weak competitive inhibitor (K_i = 450 μM) of the ADP phosphorylation, whereas the *Sp*-ADPαB isomer is a weak non-competitive inhibitor (K_i = 2.7 mM). The efficiency of ADP phosphorylation by PK, here in the presence of Mn^{2+} ($K_{m\,ADP}$ = 240 μM, k_{cat} = 150 s^{-1}), is comparable to that reported in the literature in the presence of Mg^{2+} ($K_{m\,ADP}$ = 390 μM, k_{cat} = 288 s^{-1}) [49].

Table 1
Creatine kinase—NDP equilibrium dissociation constants (K_{d1}, K_{d2}), and difference in free energy levels ($\Delta\Delta G_b$) for direct[a] and TSAC[b] binding

	Direct binding[a]			TSAC binding[b]		
	K_{d1} (μM)	K_{d2} (μM)	$\Delta\Delta G_b$ (kJ/mol)	K_{d1} (μM)	K_{d2} (μM)	$\Delta\Delta G_b$ (kJ/mol)
ADP	89 ± 22	181 ± 16	0	11 ± 4	51 ± 10	0
AMP(CH_2)P[c]	31	331	−2.6	38	100	+3.1
Sp-ADPαB	34 ± 2	417 ± 152	−2.4	315 ± 56	1500 ± 170	+8.3
Rp-ADPαB	291 ± 50	2928 ± 436	+2.9	816 ± 148	5250 ± 1280	+10.7
2′-dADP	149 ± 19	288 ± 61	+1.3	111 ± 13	145 ± 53	+5.7
GDP	163 ± 53	571 ± 179	+1.5	170 ± 20	488 ± 45	+6.8
2′-dGDP	155 ± 5	615 ± 110	+1.4	258 ± 62	500 ± 88	+7.8
CDP	150 ± 53	1137 ± 389	+1.3	233 ± 83	1601 ± 682	+7.6
2′-dCDP	261 ± 38	1800 ± 424	+2.7	115 ± 20	1220 ± 139	+5.8

All experiments were performed in triplicate and reported as averages and standard deviations.
[a] One micromolar CK in 50 mM Bicine, 5 mM $MgCl_2$, and 50 mM KCl at pH 8.3 was titrated with 0–2 mM NDP at 25 °C.
[b] One micromolar CK in 50 mM Bicine, 5 mM $MgCl_2$, 50 mM $NaNO_3$, and 20 mM creatine at pH 8.3 was titrated with 0–2 mM NDP at 25 °C.
[c] One trial only.

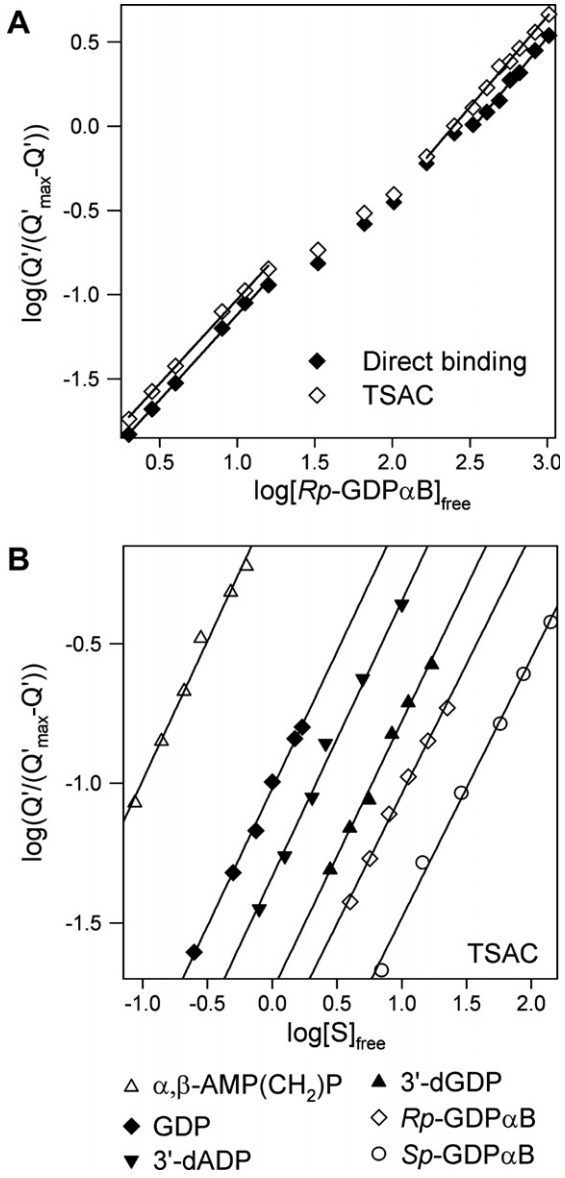

Fig. 4. (A) Hill plot of the *Rp*-GDPαB isomer for (◆) direct binding and (◇) TSAC binding with PK. (B) First binding mode of NDPs ((△) α,β-AMP(CH_2)P, (▼) 3′-dADP, (◆) GDP, (▲) 3′-dGDP, (◇) *Rp*-GDPαB, (○) *Sp*-GDPαB) bound to PK in TSAC. PK (0.2–0.7 μM) in direct binding buffer (50 mM Hepes, 5% glycerol, 5 mM $MgCl_2$, 2 mM sodium oxalate, and 100 mM KCl at pH 7.5) or TSAC binding buffer (50 mM Hepes, 5% glycerol, 5 mM $MgCl_2$, 2 mM sodium oxalate, and 50 mM KNO_3 at pH 7.5) was titrated with 0–2 mM NDP at 25 °C. Experiments were performed in triplicate.

4. Discussion

Structure–activity relationships for creatine kinase and pyruvate kinase (Fig. 7) were established based on the equilibrium dissociation constants of direct binding and nitrate TSAC (Fig. 2) binding for a wide range of nucleobase, ribose, and α-phosphate modified NDPs and NTPs. All substrate analogs have two binding modes (Figs. 3 and 4), with Hill coefficients approaching 1.0 at very high and very low substrate concentrations, and an intermediate negatively cooperative step with Hill coefficients ranging from 0.5 to 0.8. The distinct dissociation constants for each binding mode indicates allosteric behavior of the enzyme [50–52]. Both CK and PK exhibit a 2- to 10-fold lower binding affinity of the second substrate molecule, particularly for unnatural substrates, as compared to the binding affinity of the first substrate molecule ($K_{d1} < K_{d2}$). This observation is consistent with the proposition that CK and PK both display negative cooperativity with respect to substrate binding [50–52]. It is hypothesized that the binding of the first substrate molecule to the CK dimer, or PK tetramer, changes the conformation of one subunit of the enzyme which in turn affects the stability of the neighboring subunit conformation and decreases the affinity of the second substrate molecule for the vacant substrate binding site.

Whereas several studies have reported allosteric behavior of the subunits in CK, with results showing negative cooperativity or non-identical active sites [39,53–57], other studies suggest the contrary and support a non-cooperative binding behavior [40]. The fluorescence quenching approach used in our study to determine the affinity for a wide range of NDPs was previously used by Borders et al. to determine the affinity for each of the components involved in the binding of ADP to the nitrate TSAC [38]. The intrinsic dissociation constants determined by Borders et al. for direct binding (K_d = 135 μM) and TSAC binding (K_d = 14 μM) of ADP to CK correlate well with the dissociation constants for ADP determined in our study for the first binding mode ($K_{d1\,DB}$ = 89 μM, $K_{d1\,TSAC}$ = 11 μM) (Table 1).

Our studies also show that PK demonstrates a negatively cooperative binding behavior. Although this is a tetrameric enzyme and thus has four potential binding modes, only the first two binding modes were identified for PK.

Fig. 7A and B display the structure–activity relationships for CK and PK, respectively, and the binding interactions between the enzymes and ADP in their corresponding TSACs. After determining dissociation constants for a wide range of substrates a quantitative characterization of each enzyme–substrate interaction and an evaluation of its importance for binding affinity could be made. The differences in free energy change ($\Delta\Delta G_b$) upon substitutions on base, sugar, and α-phosphate from the natural substrates (ADP or ATP) are noted in Fig. 7.

Table 2
Pyruvate kinase—NDP equilibrium dissociation constants (K_{d1}, K_{d2}), and difference in free energy levels ($\Delta\Delta G_b$) for direct[a] and TSAC[b] binding

	Direct binding[a]			TSAC binding[b]		
	K_{d1} (μM)	K_{d2} (μM)	$\Delta\Delta G_b$ (kJ/mol)	K_{d1} (μM)	K_{d2} (μM)	$\Delta\Delta G_b$ (kJ/mol)
ADP	5.7 ± 1.2	789 ± 105	0	2.3 ± 0.4	632 ± 49	0
AMP(CH_2)P	5.6 ± 1.4	871 ± 132	−0.04	0.4 ± 0.1	182 ± 33	−4.3
Rp-ADPαB	68 ± 6.5	555 ± 93	+6.1	36 ± 6	721 ± 75	+6.8
Sp-ADPαB	46 ± 11	635 ± 102	+5.2	79 ± 18	737 ± 68	+8.5
2′-dADP	37 ± 4.5	611 ± 81	+4.6	29 ± 4	198 ± 35	+6.3
3′-dADP	33 ± 5	151 ± 18	+4.4	21 ± 3	141 ± 41	+5.5
GDP	22 ± 4	604 ± 59	+3.3	11 ± 3	427 ± 74	+3.9
Rp-GDPαB	108 ± 12	633 ± 85	+7.3	102 ± 6	361 ± 65	+9.4
Sp-GDPαB	132 ± 15	403 ± 58	+7.8	182 ± 42	363 ± 47	+10.8
2′-dGDP	27 ± 5	315 ± 46	+3.9	45 ± 10	471 ± 13	+7.4
3′-dGDP	24 ± 4	217 ± 39	+3.6	57 ± 8	381 ± 44	+8.0

All experiments were performed in triplicate and reported as averages and standard deviations.
[a] 0.2 (G derivatives) or 0.7 μM (A derivatives) PK in 50 mM Hepes, 5% glycerol, 5 mM $MgCl_2$, 2 mM sodium oxalate, and 100 mM KCl, at pH 7.5 was titrated with 0–2 mM NDP at 25 °C.
[b] 0.2 (G derivatives) or 0.7 μM (A derivatives) PK in 50 mM Hepes, 5% glycerol, 5 mM $MgCl_2$, 2 mM sodium oxalate, and 50 mM KNO_3, at pH 7.5) was titrated with 0–2 mM NDP at 25 °C.

Table 3
Creatine kinase—NTP direct binding equilibrium dissociation constants (K_{d1}, K_{d2}), and difference in free energy levels ($\Delta\Delta G_b$)[a]

	Direct binding[a]		
	K_{d1} (μM)	K_{d2} (μM)	$\Delta\Delta G_b$ (kJ/mol)
ATP	77 ± 20	1900 ± 173	0
2′-dATP	125 ± 38	379 ± 39	+1.2
3′-dATP	299 ± 91	1600 ± 424	+3.4
2′3′-ddATP	58 ± 25	482 ± 243	−0.7
GTP	249 ± 28	446 ± 129	+2.9
2′-dGTP	285 ± 10	562 ± 18	+3.2
2′3′-ddGTP	98 ± 20	508 ± 155	+0.6
CTP	260 ± 47	1252 ± 357	+3.0
2′-dCTP	281 ± 56	930 ± 396	+3.2
2′3′-ddCTP	159 ± 51	694 ± 67	+1.8

[a] One micromolar CK in 50 mM Bicine, 5 mM $MgCl_2$, and 50 mM KCl at pH 8.3 was titrated with 0–2 mM NDP at 25 °C. Experiments were performed in triplicate and reported as averages and standard deviations.

Table 4
Steady-state kinetic and inhibitory constant values for the phosphorylation of NDPs by CK and PK[a]

	K_m (μM)	k_{cat} (s^{-1})	k_{cat}/K_m (M^{-1} s^{-1})	K_i (μM)
Creatine kinase				
ADP	67 ± 10	370 ± 15	5×10^6	—
Sp-ADPαB	8 ± 3	0.03 ± 0.002	4×10^3	49 ± 15
Rp-ADPαB	1000 ± 350	0.06 ± 0.02	6×10^1	[b]
Pyruvate kinase				
ADP	240 ± 85	150 ± 31	6×10^5	—
Sp-ADPαB	[c]	[c]	[c]	2700 ± 305
Rp-ADPαB	[c]	[c]	[c]	450 ± 67

Each experiment was performed in triplicate. See materials and methods for experimental conditions.
[a] K_m is the Michaelis–Menten dissociation constant, k_{cat} is mol of substrate turned over per mol of enzyme per second, the ratio of k_{cat}/K_m is the enzyme efficiency, and K_i is the inhibitory constant of ADPαB for the natural ADP reaction.
[b] No inhibition observed.
[c] Phosphorylation was too low to be measured.

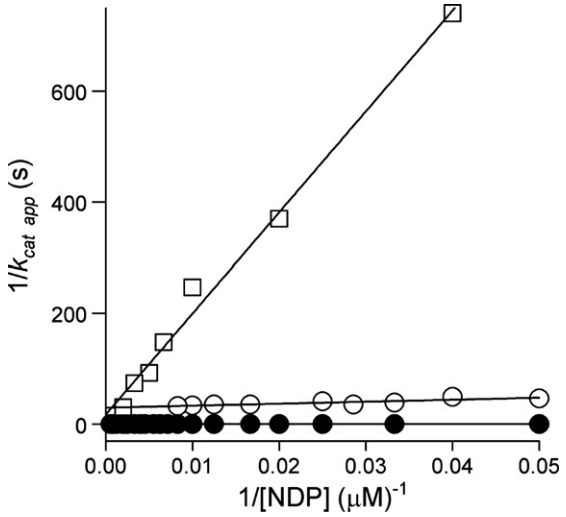

Fig. 5. Lineweaver–Burk plot for phosphorylation of (●) ADP and the (○) *Sp*-and (□) *Rp*-stereoisomers of ADPαB by creatine kinase. Reaction conditions: 0–2 mM NDP in 50 mM Bicine, 5 mM $MgCl_2$, 50 mM KCl, and 20 mM creatine phosphate at pH 8.3 and 25 °C. Optimized enzyme concentrations [CK] and reaction times (t) were as follows for ADP: [CK] = 6 nM, t = 2 min; *Sp*-ADPαB: [CK] = 600 nM, t = 15 min; and *Rp*-ADPαB: [CK] = 2 μM, t = 70 min. Each experiment was done in triplicate.

4.1. Effect of ribose and nucleobase substitution

We found that a single substitution on the ribose (2′ or 3′) or on the nucleobase (C or G) in ADP/ATP decreases the binding affinity for both CK and PK (Tables 1–3). However, for CK, NTPs bind with affinities in the order of 2′,3′-ddATP ⩾ ATP > 2′-dATP > 3′-dATP (Table 3). The removal of the ribose 2′ hydroxyl group decreases the binding affinity, as does the removal of the 3′ hydroxyl group. However, substitution of both 2′ and 3′ hydroxyl groups for hydrogens (resulting in dideoxy NTP) increases the affinity of the substrate for CK (Table 3). These results indicate that 2′,3′-ddATP may be a preferred substrate for CK. Guanosine and cytidine derivatives show similar trends where the NTPs bind with affinities in the order of 2′,3′-ddGTP > GTP > 2′-dGTP and 2′,3′-ddCTP > CTP > 2′-dCTP (Table 3). These results are in agreement with previously published data which show that the pyrimidine ddNDPs are substrates for CK [5]. The finding that the lack of both 2′ and 3′ ribose hydroxyl groups enhances CK binding requires further investigation. For PK, the 2′,3′-ddNTPs did not show increased affinity compared to the parent NTP.

4.2. Effect of bridging oxygen substitution

The substitution of the bridging oxygen in ADP by a methylene group, as in AMP(CH_2)P (Fig. 1), results in a greater affinity for both CK and PK (Tables 1 and 2), perhaps because the methylene group

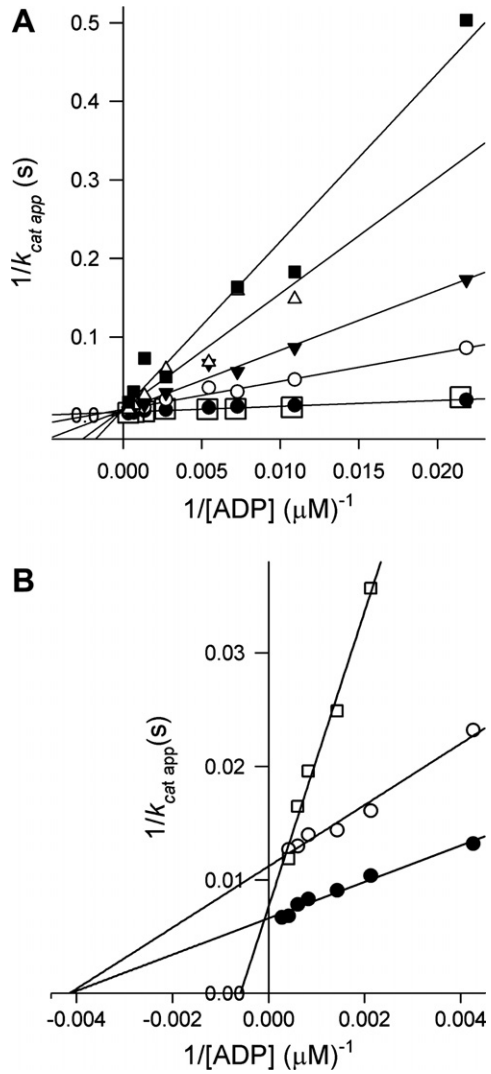

Fig. 6. Lineweaver–Burk plot for (A) *Sp*-ADPαB ((○) 100 μM, (▼) 200 μM, (Δ) 400 μM, and (■) 600 μM) competitive inhibition of (●) ADP phosphorylation by CK. No inhibition was observed with (□) *Rp*-ADPαB. Reaction conditions: 0–2 mM ADP, [*I*] = *Sp*-ADPαB: 0–600 μM in 50 mM Bicine, 5 mM $MgCl_2$, 50 mM KCl, and 20 mM creatine phosphate at 25 °C at pH 8.3. [CK] = 6 nM, *t* = 2 min. (B) (□) *Rp*-ADPαB competitive inhibition and (○) *Sp*-ADPαB non-competitive inhibition of (●) ADP phosphorylation by PK. Reaction conditions: 0–3 mM ADP, [*I*] = *Rp*-ADPαB: 1.6 mM, and [*I*] = *Sp*-ADPαB: 1.9 mM in 100 mM Hepes, 125 mM KCl, 3 mM $MnCl_2$, 3% glycerol, and 2.5 mM phosphoenolpyruvate at pH 7.5. [PK] = 1.5 nM, *t* = 30 s.

replaces the bridging oxygen (between the α- and β-phosphate in ADP), which does not seem to have any binding interactions with either enzyme (Fig. 7A and B). This observation is in accordance with previous studies that show α,β-methylene analogs of ADP and ATP can act as substrates for CK [59].

4.3. Stereospecificity of CK and PK for α-P-borano NDP isomers

The *Sp*-ADPαB isomer shows an increased binding affinity for CK for direct binding relative to ADP ($\Delta\Delta G_b = -2.4$ kJ/mol) (Table 1) but a significantly lower affinity for the TSAC than direct binding. This may be due to a lack of H-bonding interactions between the BH_3^- group and the enzyme which appears to be important for the TSAC affinity. The oxygen, replaced by BH_3^- in ADPαB, may form hydrogen bonds with R320 amine and V325 amide (Fig. 7A), whereas BH_3^- cannot form typical H bonds [27]. It is notable that, in direct binding with CK (without the presence of NO_3^- and creatine), these binding interactions seem less important and the α-*P*-borano substitution increases the affinity relative to the natural ADP substrate. Conversely, the *Rp* isomer is a poor substrate in both direct binding and TSAC formation with CK, possibly due to a lack of interaction of the borane with the Mg^{2+} ion. CK clearly shows stereospecificity toward the *Sp* isomer of ADPαB, where the phosphoryl oxygen can interact with Mg^{2+}.

PK shows opposite stereospecificity. For all of the studied NDPαB substrate analogs, a greater TSAC affinity is observed for the *Rp* isomer over the *Sp* isomer (Table 2). The opposite stereospecificity of CK and PK may be explained by the interaction (or lack thereof) with Mg^{2+}. Divalent metal ions have been shown to be essential in phosphoryl transfer reactions [60]. Mg^{2+} plays an important role in the substrate binding process by decreasing electrostatic repulsion and stabilizing the transition state. When the *Rp*-ADPαB isomer binds to CK, the BH_3^- group replaces the oxygen on the α-phosphorus that interacts with Mg^{2+}. The BH_3^- group most likely does not interact with the Mg^{2+} ion [27] and hence the affinity of the *Rp* isomer for CK significantly decreases. The Mg^{2+} ion plays a similar role in PK substrate binding, with the difference that the chelating Mg^{2+} is placed on the opposite side at the active site (Fig. 7B). Therefore, the *Sp* isomer BH_3^- group replaces the oxygen (on the α-phosphorus) that interacts with Mg^{2+} and the resultant limited interaction may cause a decrease in affinity.

These results are in accordance with previous studies that reported CK stereospecificity toward the *Rp*-ATPαS isomer, which has an S^- substitution in place of the oxygen interacting with Mg^{2+} [33] and has the same configuration as the *Sp*-ATPαB isomer.

In an effort to better understand the mechanism of phosphorylation of ADP and the stereoisomers of ADPαB, the phosphorylation reactions were studied using steady-state kinetics. Both isomers of ADPαB are minimally phosphorylated by CK. Notably, the natural substrate (ADP) of CK is phosphorylated 1000 times more efficiently than the *Sp*-ADPαB isomer. However, significant stereospecificity is observed, as the *Sp*-ADPαB isomer is phosphorylated 70 times more efficiently than the *Rp*-ADPαB isomer. By contrast, for PK, no measurable phosphorylation of either ADPαB stereoisomer is observed.

4.4. Stereospecific inhibition of CK and PK

The *Sp*-ADPαB isomer is a strong competitive inhibitor of the ADP reaction catalyzed by CK (Table 4). The *Sp*-ADPαB isomer seems to bind to CK at the active site but the enzyme may not adapt to the configuration necessary for efficient catalysis. However, with the *Rp*-ADPαB isomer, no inhibition is observed. The *Rp* isomer does not bind or adapt to the transition state efficiently probably due to the α-*P*-borano substitution eliminating the ability to chelate the Mg^{2+} ion. For PK, the *Rp*-ADPαB isomer is a weak competitive inhibitor of the ADP phosphorylation, whereas the *Sp*-ADPαB isomer is a weak non-competitive inhibitor. Interestingly, PK exhibits opposite stereospecificity than CK. Here, the *Rp* isomer of ADPαB seems to bind, as a weak competitive inhibitor, to the active site of PK but is not phosphorylated with any measurable efficiency. The *Sp* isomer, however, likely binds as a weak non-competitive inhibitor at a different location than the active site on PK and hence is not phosphorylated.

5. Conclusion

In summary, the affinity studies performed here confirm the observation that CK and PK play a role in the phosphorylation of acyclo- and dideoxy-nucleoside diphosphate analogs, as a greater affinity is observed with ddNTPs than the parent NTPs for CK

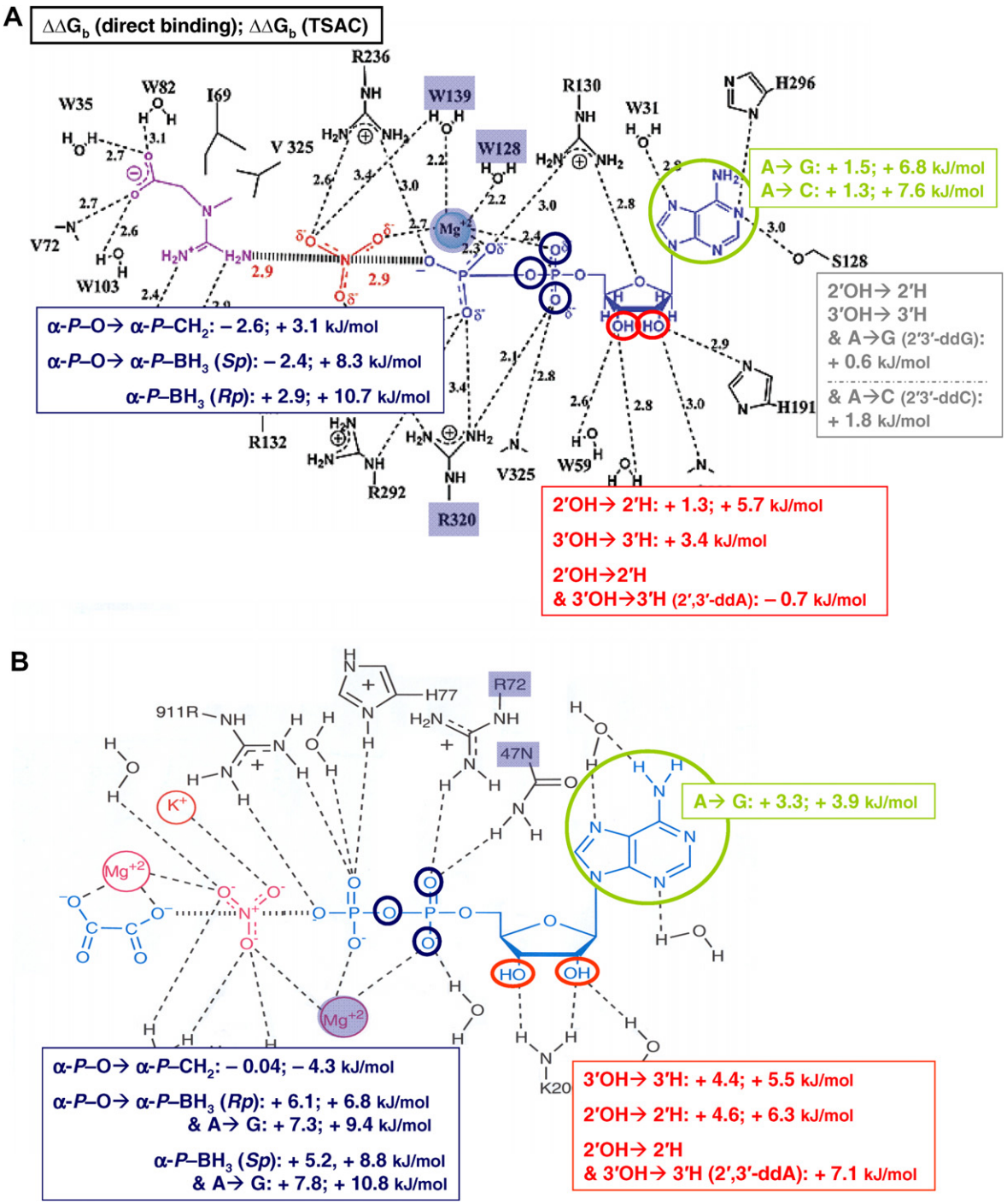

Fig. 7. Structure–activity relationships for CK (A) and PK (B). The differences in free energy change ($\Delta\Delta G_b$) upon substitutions on base (C or G), sugar (2′-deoxy, 3′-deoxy, or 2′,3′-dideoxy) and α-phosphate (α-*P*-CH_2 or α-*P*-BH_3^- relative to the natural substrates (ADP or ATP) are listed in the figure (first value corresponds to direct binding $\Delta\Delta G_b$ and the second value to the TSAC $\Delta\Delta G_b$). The ChemDraw figures of the active site of the CK-TSAC and PK-TSAC structures were adapted from Lahiri et al. and Larsen et al. [46,58] (distances in angstroms).

(see Fig. 7). Nucleobase or ribose substitutions from ADP are otherwise not preferred for either CK or PK binding. Both enzymes, however, display a negatively cooperative binding behavior for all NDP and NTP substrates and show a greater affinity for adenosine methylene diphosphonate. For CK, the α-*P*-borano substituted ADP is phosphorylated 1000-fold less efficiently than ADP and the enzyme is significantly stereospecific for the *Sp* isomer of ADPαB. PK shows opposite stereospecificity by demonstrating a preference for the *Rp* isomer of NDPαBs in the TSAC. The inhibition studies reveal that the *Sp* isomer of ADPαB is a strong competitive inhibitor for CK. For PK, the *Rp*-ADPαB isomer is a poor competitive inhibitor and the *Sp*-ADPαB isomer is a poor non-competitive inhibitor. Moreover, no significant inhibition was observed for the *Rp* isomer of ADPαB for either enzyme. This is important as the *Rp* isomer of α-*P*-borano substituted ddNTP analogs has shown promising antiviral activity and candidates for therapy should not inhibit host enzymes. The study described in this paper is useful as it provides insight into the stereospecific properties of pyruvate and creatine kinases and also their specificities for ribose, base and α-phosphate substrate modifications.

Acknowledgments

This work was supported by NIH Grant R01 AI52061 to B.R.S. and by Charles Bradsher and Kathleen Zielek Duke University graduate fellowships to C.K.W.

Appendix A. Supplementary data

Supplementary data associated with this article can be found, in the online version, at doi:10.1016/j.bioorg.2008.03.001.

References

[1] J. Bourdais, R. Biondi, S. Sarfati, C. Guerreiro, I. Lascu, J. Janin, M. Véron, J. Biol. Chem. 271 (1996) 7887–7890.
[2] P. Meyer, B. Schneider, S. Sarfati, D. Deville-Bonne, C. Guerreiro, J. Boretto, J. Janin, M. Véron, B. Canard, EMBO J. 19 (2000) 3520–3529.
[3] B. Schneider, R. Sarfati, D. Deville-Bonne, M. Véron, J. Bioenerg. Biomembr. 32 (2000) 317–324.
[4] B. Selmi, J. Boretto, S.R. Sarfati, C. Guerreiro, B. Canard, J. Biol. Chem. 276 (2001) 48466–48472.
[5] P. Krishnan, Q. Fu, W. Lam, J. Liou, G. Dutschman, Y. Cheng, J. Biol. Chem. 277 (2002) 5453–5459.
[6] A.R. Van Rompay, M. Johansson, A. Karlsson, Pharmacol. Ther. 87 (2000) 189–198.
[7] L. Placidi, E. Cretton-Scott, G. Gosselin, C. Pierra, R.F. Schinazi, J.-L. Imbach, M.H. Kouni, J.-P. Sommadossi, Antimicrob. Agents Chemother. 44 (2000) 853–858.
[8] J.E. Reardon, R.C. Crouch, L.S. John-Williams, J. Biol. Chem. 269 (1994) 15999–16008.
[9] N. Sluis-Cremer, D. Arion, M.A. Parniak, Cell. Mol. Life Sci. 57 (2000) 1408–1422.
[10] J. Deval, B. Selmi, J. Boretto, M.P. Egloff, C. Guerreiro, S. Sarfati, B. Canard, J. Biol. Chem. 277 (2002) 42097–42104.
[11] H. Huang, R. Chopra, G.L. Verdine, S.C. Harrison, Science 282 (1998) 1669–1675.
[12] L. Menendez-Arias, Trends Pharmacol. Sci. 23 (2002) 381–388.
[13] P. Li, M.I. Dobrikov, H. Liu, B.R. Shaw, Org. Lett. 5 (2003) 2401–2403.
[14] M. Dobrikov, Z. Sergueeva, B.R. Shaw, Nucleosides Nucleotides Nucleic Acids 22 (2003) 1651–1655.
[15] J. Tomasz, B.R. Shaw, K. Porter, B.F. Spielvogel, A. Sood, Angew. Chem. Int. Ed. 31 (1992) 1373–1375.
[16] K. He, K.W. Porter, A. Hasan, J.D. Briley, B.R. Shaw, Nucl. Acid Res. 27 (1999) 1788–1794.
[17] B.R. Shaw, J. Wan, X. Wang, M. Dobrikov, K. He, K. Porter, J.L. Lin, V. Rait, D. Sergueev, Z. Sergueeva, in: Collection Symposium series, 2002, pp. 169–180.
[18] J.S. Summers, B.R. Shaw, Curr. Med. Chem. 8 (2001) 1147–1155.
[19] K. He, A. Hasan, B. Krzyzanowska, B.R. Shaw, J. Org. Chem. 63 (1998) 5769–5773.
[20] A. Sood, B.R. Shaw, B.F. Spielvogel, J. Am. Chem. Soc. 112 (1990) 9000–9001.
[21] B.R. Shaw, D. Sergueev, K. He, K. Porter, J. Summers, Z. Sergueeva, V. Rait, Methods Enzymol.: Antisense Technol. 313 (2000) 226–257.
[22] K.W. Porter, J.D. Briley, B.R. Shaw, Nucleic Acids Res. 25 (1997) 1611–1617.
[23] B.R. Shaw, J. Madison, A. Sood, B.F. Spielvogel, in: S. Agrawal, Methods in Molecular Biology Series 20, 1993, pp. 225–243.
[24] B.K. Krzyzanowska, K. He, A. Hasan, B.R. Shaw, Tetrahedron 54 (1998) 5119–5128.
[25] V. Nahum, B. Fischer, Eur. J. Inorg. Chem. 20 (2004) 4124–4131.
[26] P. Li, Z.A. Sergueeva, M. Dobrikov, B.R. Shaw, Chem. Rev. 107 (2007) 4746–4796.
[27] J.S. Summers, D. Roe, P.D. Boyle, M. Colvin, B.R. Shaw, Inorg. Chem. 37 (1998) 4158–4159.
[28] B.R. Shaw, M.I. Dobrikov, X. Wang, J. Wan, K. He, J.-L. Lin, P. Li, V. Rait, Z. Sergueeva, D. Sergueev, Ann. N. Y. Acad. Sci. 1002 (2003) 12–29.
[29] M.I. Dobrikov, K.M. Grady, B.R. Shaw, Nucleosides Nucleotides Nucleic Acids 22 (2003) 275–282.
[30] P. Li, B.R. Shaw, Nucleosides Nucleotides Nucleic Acids 22 (2003) 699–701.
[31] P. Li, B.R. Shaw, Nucleosides, Nucleotides Nucleic Acids 24 (2005) 675–678.
[32] S. Gallois-Montbrun, B. Schneider, Y. Chen, V. Giacomoni-Fernandes, L. Mulard, S. Morera, J. Janin, D. Deville-Bonne, M. Véron, J. Biol. Chem. 277 (2002) 39953–39959.
[33] F. Eckstein, R. Goody, Biochemistry 15 (1976) 1685–1691.
[34] T.D. Wallimann, M. Dolder, U. Schlattner, M. Eder, T. Hornemann, E. O'Gorman, A. Ruck, D. Brdiczka, Biofactors 8 (1998) 229–234.
[35] V.A. Saks, Z.A. Khuchua, E.V. Vasilyeva, O.Y. Belikova, A.V. Kuznetsov, Mol. Cell. Biochem. 133–134 (1994) 155–192.
[36] T. Walliman, W. Hemmer, Mol. Cell. Biochem. 133–134 (1994) 193–220.
[37] E.J. Milner-White, D.C. Watts, Biochem. J. 122 (1971) 727–740.
[38] C.L. Borders, M. Snider, R. Wolfenden, P. Edmiston, Biochemistry 41 (2002) 6995–7000.
[39] S.D. Lahiri, P.-F. Wang, P.C. Babbit, M.J. McLeish, G.L. Kenyon, K.N. Allen, Biochemistry 41 (2002) 13861–13867.
[40] H. Mazon, O. Marcillat, E. Forest, C. Vial, Biochemistry 42 (2003) 13596–13604.
[41] G.H. Reed, T.S. Leyh, Biochemistry 19 (1980) 5472–5480.
[42] G.H. Reed, M. Cohn, J. Biol. Chem. 247 (1972) 3073–3081.
[43] P. Li, Z. Xu, H. Liu, C.K. Wennefors, M.I. Dobrikov, J. Ludwig, B.R. Shaw, J. Am. Chem. Soc. 127 (2006) 16782–16783.
[44] S.A. Kuby, L. Noda, H.A. Lardy, J. Biol. Chem. 210 (1954) 65–82.
[45] A.S. Mildvan, M. Cohn, J. Biol. Chem. 240 (1965) 238–246.
[46] K.M. Plowman, A.R. Krall, Biochemistry 4 (1965) 2809–2814.
[47] A.M. Reynard, L.F. Hass, D.D. Jacobsen, P.D. Boyer, J. Biol. Chem. 236 (1961) 2277–2283.
[48] M.I. Dobrikov, B.R. Shaw, Nucleosides, Nucleotides Nucleic Acids 24 (2005) 983–987.
[49] R.H. Friesen, R.J. Castellani, J.C. Lee, W. Braun, Biochemistry 37 (1998) 15266–15276.
[50] A. Fersht, Structure and Mechanism in Protein Science—A Guide to Enzyme Catalysis and Protein Folding, W.H. Freeman and Company, New York, 1999.
[51] D. Piszkiewicz, Kinetics of Chemical and Enzyme-Catalyzed Reactions, Oxford University Press, New York, 1977.
[52] I.H. Segel, Enzyme Kinetics—Behavior and Analysis of Rapid Equilibrium and Steady-State Systems, John Wiley & Sons, Inc., New York, 1975.
[53] G.F. Bickerstaff, N.C. Price, Int. J. Biochem. 9 (1978) 1–8.
[54] Y. Degani, C. Degani, Biochemistry 18 (1979) 5917–5923.
[55] T. Hornemann, D. Rutishauser, T. Walliman, Biochim. Biophys. Acta 1480 (2000) 365–373.
[56] G.A. Nevinsky, V.N. Ankilova, O.I. Lavrik, Z.S. Mkrtchyan, L.S. Nersesova, J.I. Akopyan, FEBS Lett. 149 (1982) 36–40.
[57] N.C. Price, M.G. Hunter, Biochim. Biophys. Acta 445 (1976) 364–376.
[58] T.M. Larsen, M.M. Benning, I. Rayment, G.H. Reed, Biochemistry 37 (1998) 6247–6255.
[59] E.J. Milner-White, D.S. Rycroft, Eur. J. Biochem. 133 (1983) 169–172.
[60] I. Lascu, P.J. Gonin, Bioenerg. Biomembr. 32 (2000) 237–246.